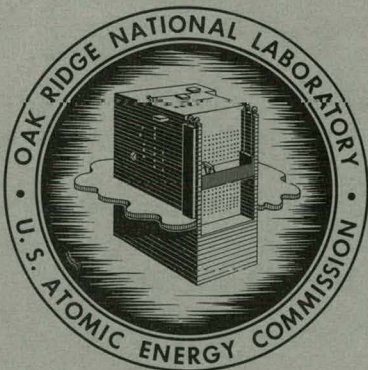325
9-21-6

ORNL-3316
UC-25 – Metals, Ceramics, and Materials
TID-4500 (17th ed., Rev.)

SPECTROPHOTOMETRIC STUDY OF DILUTE

SOLUTIONS OF BISMUTH IN MOLTEN $BiCl_3$

Charles R. Boston
G. Pedro Smith

DISCLAIMER

DISCLAIMER

Portions of this document may be illegible in electronic image products. Images are produced from the best available original document.

ORNL-3316

UC-25 — Metals, Ceramics, and Materials
TID-4500 (17th ed.)

Contract No. W-7405-eng-26

METALS AND CERAMICS DIVISION

SPECTROPHOTOMETRIC STUDY OF DILUTE SOLUTIONS
OF BISMUTH IN MOLTEN $BiCl_3$

Charles R. Boston and G. Pedro Smith

DATE ISSUED

SEP 1 8 1962

OAK RIDGE NATIONAL LABORATORY
Oak Ridge, Tennessee
operated by
UNION CARBIDE CORPORATION
for the
U. S. ATOMIC ENERGY COMMISSION

SPECTROPHOTOMETRIC STUDY OF DILUTE SOLUTIONS
OF BISMUTH IN MOLTEN BiCl₃ [1]

Charles R. Boston and G. Pedro Smith

ABSTRACT

Solute bismuth metal in chloride-rich melts of the system Bi-BiCl₃ is found to be partitioned into two chemical species which obey the law of additive absorbances. Absorption spectra from 450 to 750 mμ are reported for molten Bi-BiCl₃ mixtures 0.0027 to 0.7 molar in solute bismuth metal at path lengths as short as 24 μ and at temperatures of 264, 350, and 433°C. The spectrum consists of an intense, broad band with a maximum near 560 mμ. Large apparent deviations from Beer's law are found at all wavelengths. These spectra have the characteristics expected for solutions with two light-absorbing solute species. Phenomenological equations are derived which describe the spectra of solutions consisting of any given number of solute species derived from a common substance.

INTRODUCTION

The molecular constitution of the liquid phases of bismuth-bismuth trihalide and related metal-metal salt systems is an unsolved problem which has attracted much recent research and debate. Much of this work is reviewed elsewhere.[2-4] It is usually assumed that bismuth metal dissolves in halide-rich melts to form a single solute species. However, some workers[3-5] assert that there are two or more solute species which

---

[1]A preliminary report of this study was presented at the 137th Meeting of the American Chemical Society, Cleveland, Ohio, April, 1960, and a final report was presented at the XVIIIth International Congress of Pure and Applied Chemistry, Montreal, Canada, August, 1961; a condensed version was published in J. Phys. Chem. 66(6), 1178-81 (1962).

[2]D. Cubicciotti, J. Chem. Educ. 37, 540 (1960).

[3]S. J. Yosim et al., J. Phys. Chem. 63, 230 (1959).

[4]N. H. Nachtrieb, J. Phys. Chem. (in press).

[5]M. A. Bredig, J. Phys. Chem. 63, 978 (1959).

are in equilibrium. No specific solute species has been demonstrated
to exist in the halide-rich melts. The species which have been postulated
include such diverse entities as bismuth atoms,[6] polymers of bismuth
atoms,[7] monovalent bismuth ions and their polymers,[5-7] and "ions plus
electrons."[3] The research reported here provides spectrophotometric
evidence which clearly favors a two-species model for chloride-rich
melts of bismuth in bismuth trichloride.

EXPERIMENTAL

Materials

Bismuth trichloride was prepared by direct reaction between bismuth
metal and chlorine gas. The product was purified by distillation under
chlorine followed by purging chlorine from the melt with argon. Analysis
of the salt showed 33.68 wt % Cl as compared with the theoretical value
of 33.73%. This material was extremely sensitive to air contamination.
Therefore, all handling, including analytical weighing, was performed
in a vacuum-type dry box filled with high-purity nitrogen.

Bismuth metal, used as a solute, was deoxidized by bubbling hydrogen
through molten, reagent-grade metal held on a sintered glass disk. The
oxide-free metal was filtered through the sintered disk into a glass
tube, sealed off under vacuum, and later opened in the dry box where
the metal ingot was broken up in a mortar and placed in a weighing
bottle.

Measurements

A Cary Model 11MS spectrophotometer modified for high-temperature
work[8] was used to make the spectral measurements. Fused silica cell-
insert combinations were used to provide path lengths from 24 to 500 μ.

[6]T. K. Keneshea, Jr. and D. Cubicciotti, _J. Phys. Chem._ 62, 843
(1958); 63, 1112, 1472 (1959).

[7]J. D. Corbett, _J. Phys. Chem._ 62, 1149 (1958).

[8]C. R. Boston and G. P. Smith, _J. Phys. Chem._ 62, 409 (1958).

Cells were loaded with weighed amounts (10–12 g) of $BiCl_3$ in the dry box and held under a flow of argon during spectral measurements. Melt composition was changed between spectral scans by adding bismuth metal through the top of the cell while keeping a stream of argon passing over the melt.

The possibility that atmospheric contamination significantly influenced the spectra was excluded by the results of measurements on two Bi-$BiCl_3$ mixtures which were sealed in optical cells under 1/3 atm of argon. The spectra of these sealed mixtures were quantitatively like the spectra obtained with stoppered cells.

Nomenclature and Units

All of the melts to be considered lie at the $BiCl_3$-rich end of the Bi-$BiCl_3$ binary system. Accordingly, pure $BiCl_3$ will be referred to as the solvent and the amount of bismuth in excess of that in pure $BiCl_3$ will be referred to as solute bismuth. The concentration of solute bismuth in moles per liter of melt is calculated from the composition by weight on the basis of the density measurements of Keneshea and Cubicciotti[6] and is denoted $\underline{M}_f$. This is a "formal" measure of solute concentration which may or may not equal the molar concentrations of the atomic, molecular, or ionic species in which the solute bismuth exists in the solution.

The absorbance $\underline{A}$ of a solution is defined in the usual way as $\log_{10} [\underline{I}(solv)/\underline{I}(soln)]$. In practice, the absorption of the solvent and the solution were measured separately with an air reference as functions of wavelength using the same cell under the same conditions. Then the absorbance of the solution was calculated by subtraction.

The data were recorded as binary numbers punched into paper tape by means of high-precision recording devices. Calculations including the above subtraction were done by a digital computer which read directly the paper-tape output of the spectrophotometer. In the recording operation, absorbance values were sampled at 1-mμ intervals.

The extinction coefficient (molar absorptivity) ϵ of a single solute species is defined in the usual way by the relation $\epsilon = \underline{A}/\underline{bM}$ where $\underline{A}$ and $\underline{M}$ are the absorbance and molarity, respectively, ascribed to a

specified species and $\underline{b}$ is the path length in centimeters. The formal extinction coefficient ϵ_f of a solution (which may contain several species) is defined by the relation $\epsilon_f = \underline{A}/\underline{bM_f}$, where $\underline{A}$ is the experimentally measured absorbance of the solution. If only one solute species exists, ϵ_f equals ϵ for that species.

It may be helpful to know that the composition in mole % of solute bismuth metal is about 8 to 10 times $\underline{M_f}$. The exact relation depends, of course, on the temperature and the exact M_f value.

RESULTS

The bismuth trichloride solvent was essentially transparent at wavelengths between 500 and 750 mμ but a steeply rising absorption edge occurred below 500 mμ which gave a short wavelength cutoff. Figure 1 shows the position of this edge at temperatures and path lengths frequently used in this research. From considerations of signal-to-noise ratio, it was concluded that no useful absorbance values could be determined below 400 mμ. The limiting wavelength for precise measurement varied between about 420 and 500 mμ depending on the conditions of measurement. With long path lengths (small M_f) at 433°C, the limit for precise measurement was about 500 mμ, while, with short path lengths (large M_f) at 264°C, the limit was about 420 mμ.

Typical spectra for different concentrations of bismuth at different temperatures are shown in Fig. 2 in terms of ϵ_f as functions of wavelength. The shaded strip at 264°C is a region within which lie the spectra for all solutions from 0.0141 M_f down to the lowest concentration measured, 0.0027 M_f. At low concentrations, a strong band is found. The band maximum occurs at a wavelength of about 560 mμ for 264°C and at a somewhat longer wavelength for higher temperatures. The band is skewed toward longer wavelengths and at 433°C has a slight shoulder near 610 mμ so that it may be a composite of absorptions due to more than one electronic transition. The most striking feature of the spectra is the manner in which the band diminishes with increasing M_f until it is almost indistinguishable against the background of a diffuse absorption edge which rises very slowly with shortening wavelength.
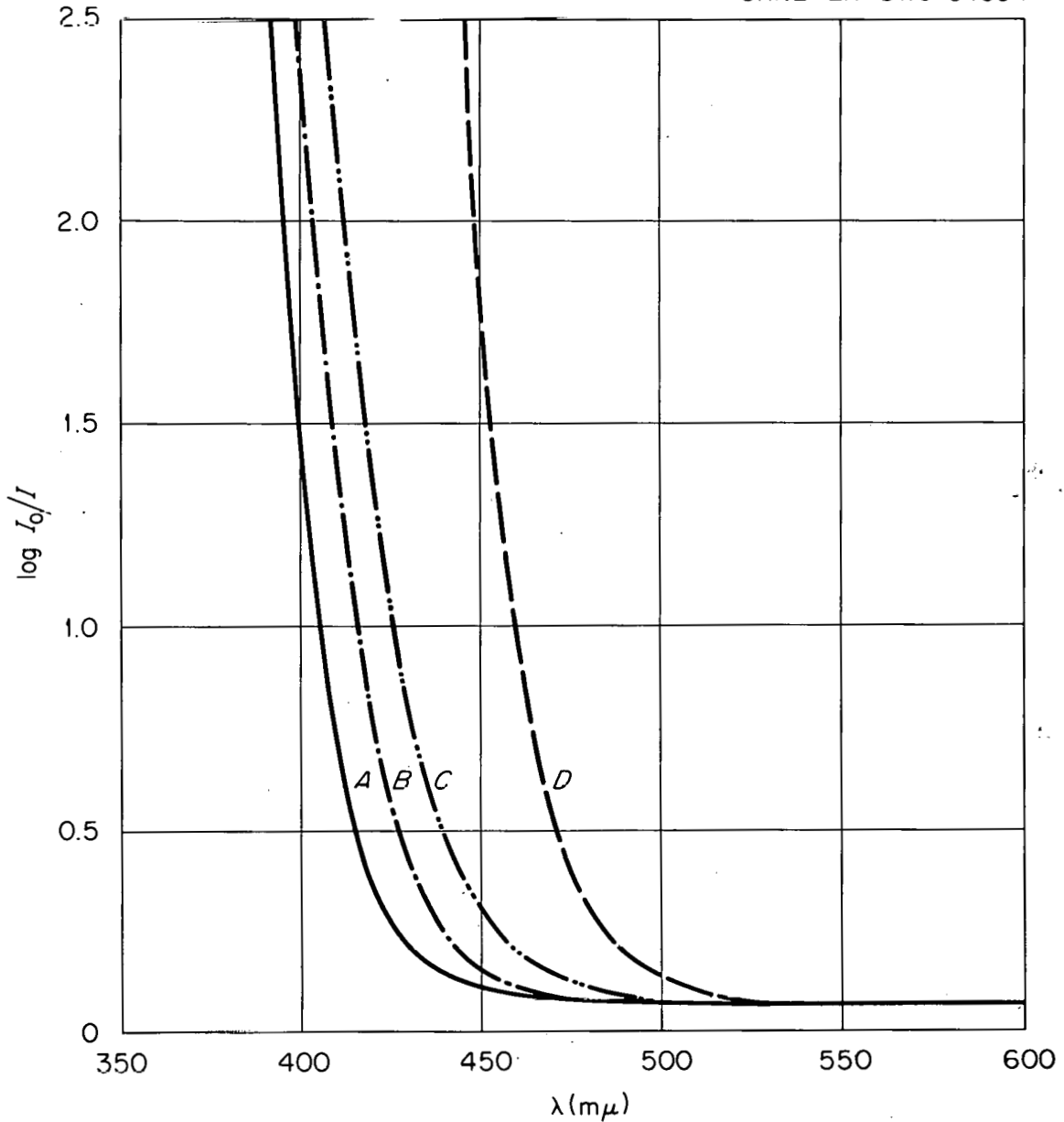
Fig. 1. Typical Absorption Spectra of Pure Molten BiCl$_3$ Plus the Silica Cell. Spectra A, B, and C are for a path length of 0.00276 cm and temperatures of 264, 350, and 433°C, respectively. Spectrum D is for a path length of 0.0501 cm and a temperature of 350°C.
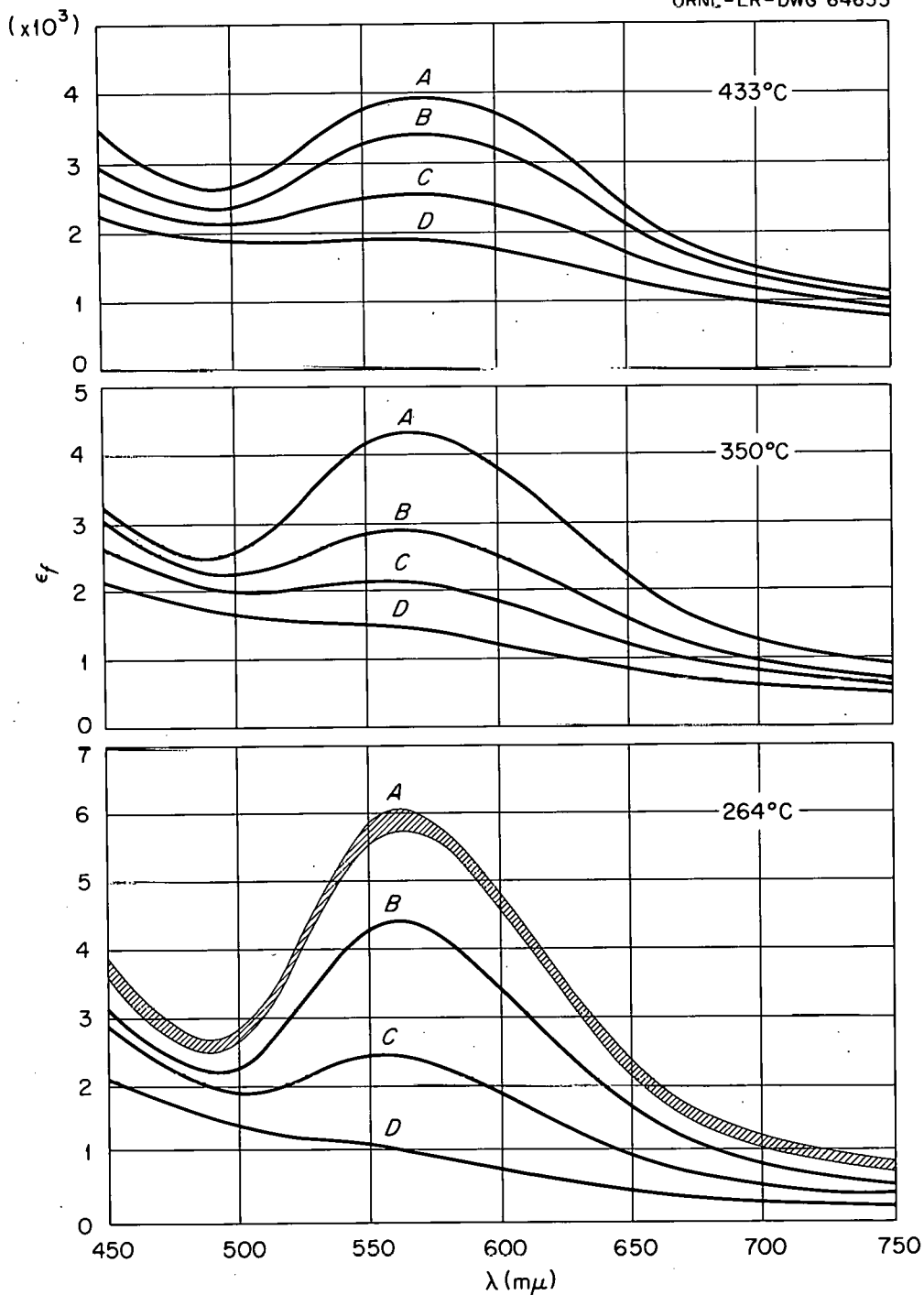
Fig. 2. Typical Spectra of Molten Bi-BiCl$_3$ Mixtures in Terms of ϵ_f vs λ with M_f values as follows: at 264°C, A = 0.0027 to 0.0141, B = 0.0341, C = 0.113, and D = 0.696; at 350°C, A = 0.0485, B = 0.148, C = 0.280, and D = 0.679; and at 433°C, A = 0.0099, B = 0.106, C = 0.213, and D = 0.464.

Figures 3, 4, and 5 show the manner in which A/b varies with M_f for a wavelength near the band maximum. Figure 3 shows this variation for the M_f range which was studied at each temperature while Figs. 4 and 5 show for 264 and 350°C, respectively, the data at low concentration for which A/b varies linearly with M_f. Low concentration data for 433°C scatter too much to justify a plot on an expanded scale.

The shaded strip in Fig. 2 for 264°C includes all of those spectra which lie in the linear range of A/b vs M_f as shown in Fig. 4. There is no trend with increasing M_f for the spectra within this strip. Consequently, the strip indicates the precision within which ϵ_f is known for the linear range and, likewise, the precision within which A/b vs M_f is linear at wavelengths other than that chosen for Fig. 4. A similar shaded strip could be drawn about the lowest concentration spectrum at the other two temperatures.

DISCUSSION

For solutions with a single solute species, Beer's law is generally approximated, that is, A/b is proportional to the solute concentration and the molar extinction coefficient ϵ varies with wavelength but not concentration. However, for solutions of bismuth metal in fused bismuth trichloride, it is evident from Figs. 2 and 3 that Beer's law is not even approximately obeyed save at the lowest concentrations as shown in Figs. 4 and 5. We shall show that these very large departures from Beer's law can be accounted for in a quantitative way if one assumes that the solute bismuth metal is partitioned between two solute species each of which individually obeys Beer's law, that is, a two-species solution with additive absorbances. Since we have no a priori way of knowing the molar extinction coefficients of these postulated species, we shall recast the phenomenological law of additive absorbances into a form which does not contain these coefficients.

Let us suppose that the solute bismuth dissolves in or reacts with the fused bismuth trichloride solvent to form two molecular species X_n and X_m. Conservation of mass requires that

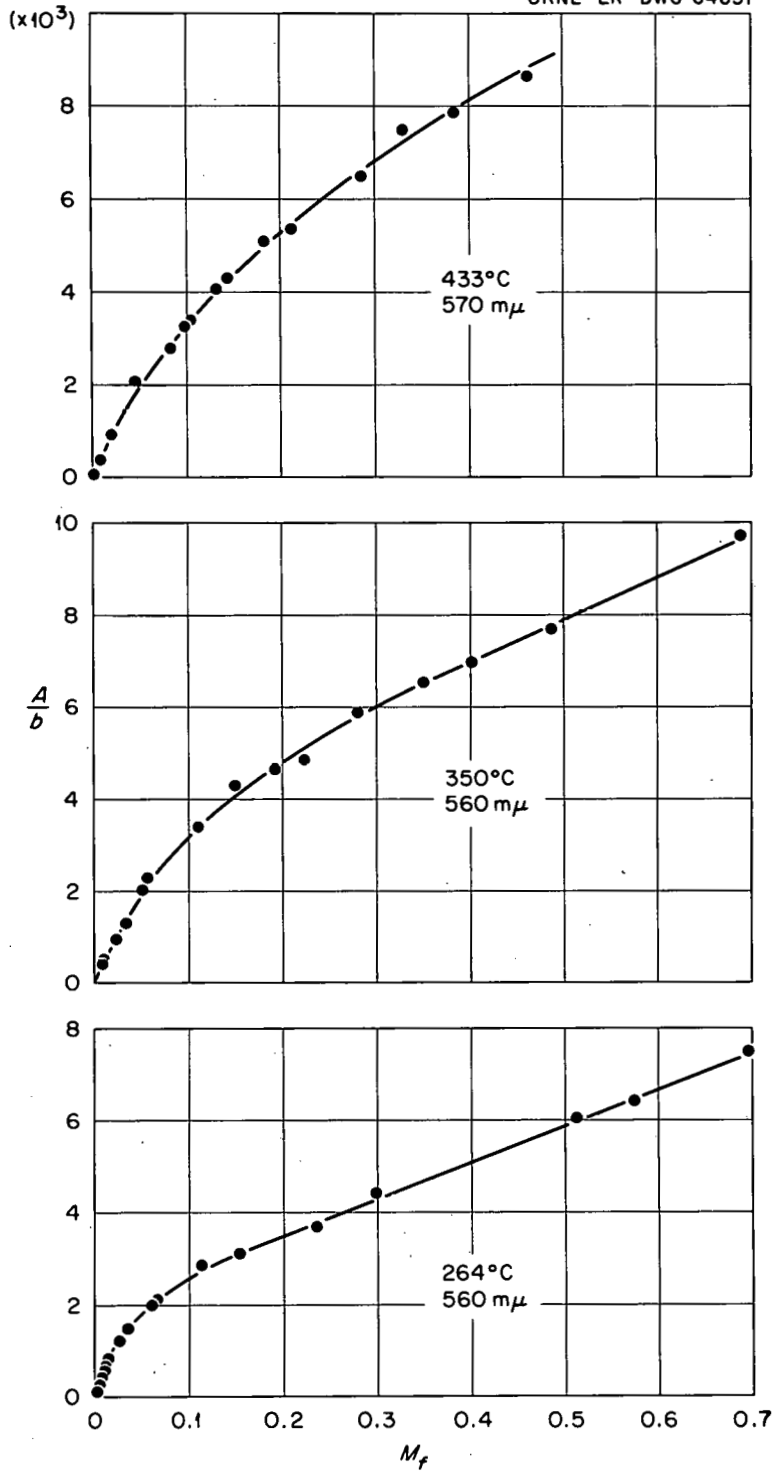$$M_f = D_n M_n + D_m M_m, \tag{1}$$

Fig. 3. Beer's Law Plots for All Values of M_f and for A/b Near the Band Maximum. At 264 and 350°C, A/b was determined at 560 mμ while at 433°C A/b was determined at 570 mμ.

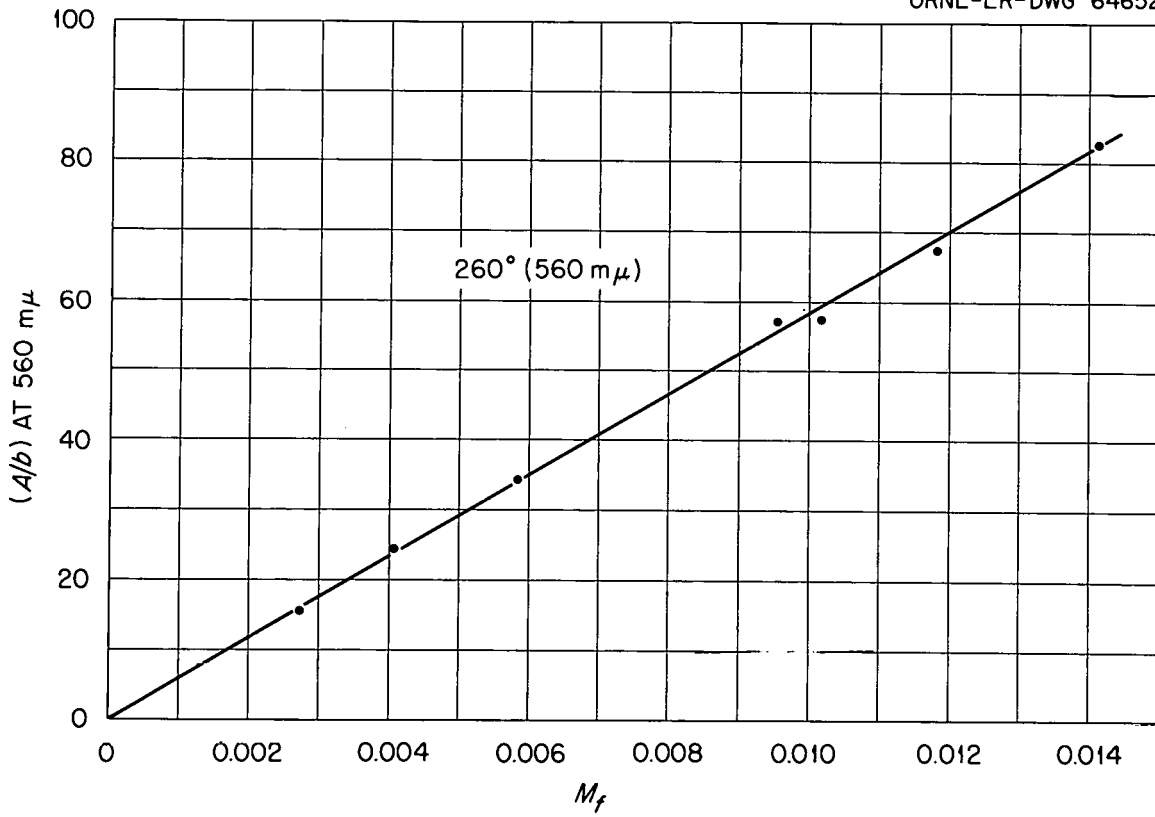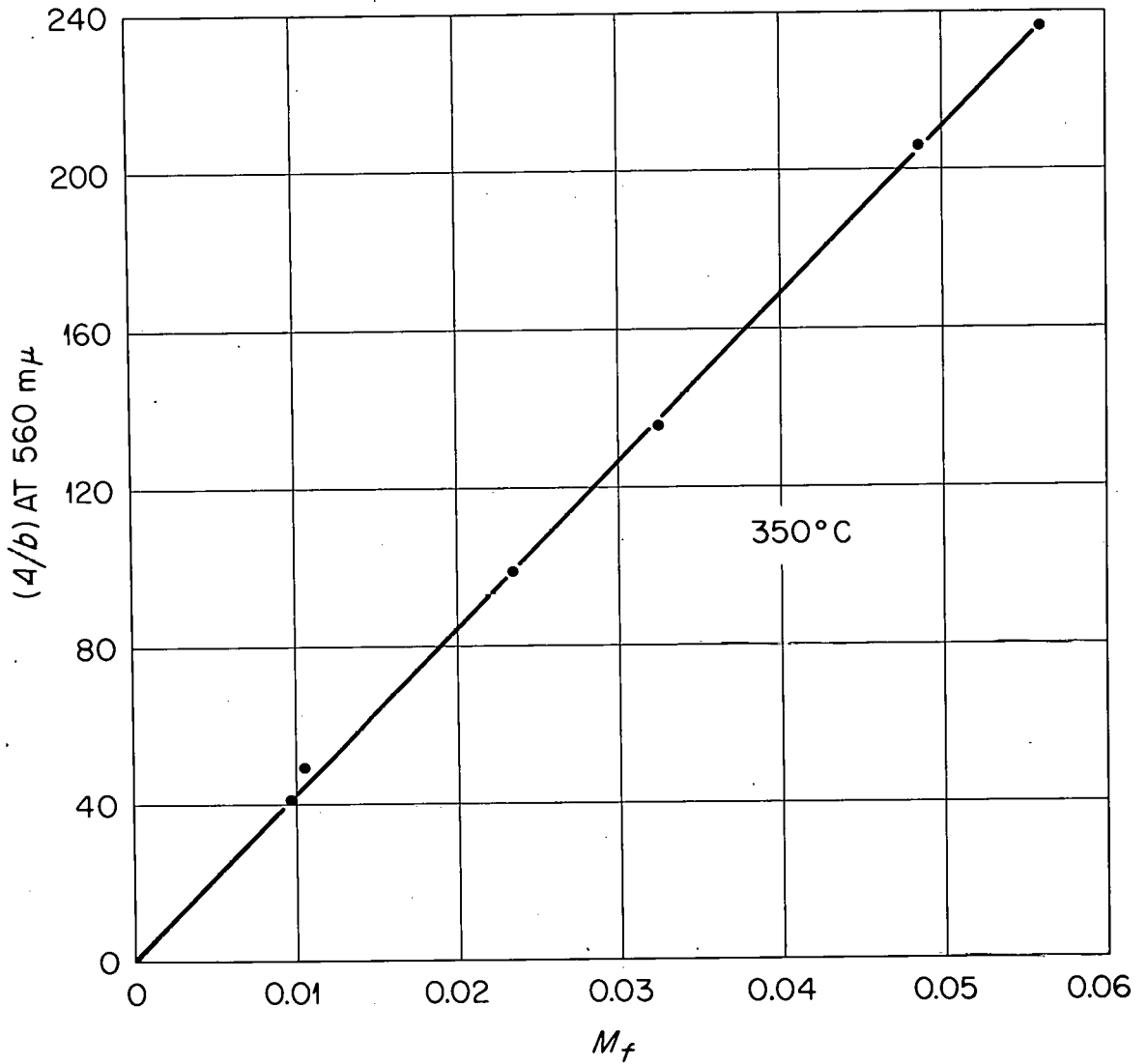Fig. 4. Beer's Law Plot for the M_f Range Over Which A/b is Linear at 264°C.

Fig. 5. Beer's Law Plot for the M_f Range Over Which A/b is Linear at 350°C.

where M_n and M_m are, respectively, the molar concentrations of X_n and X_m, and where D_n and D_m are the numbers of moles of solute bismuth required to form one mole, respectively, of X_n and X_m. The law of additive absorbances may be written

$$A/b = \epsilon_f M_f = \epsilon_n M_n + \epsilon_m M_m, \tag{2}$$

where ϵ_n and ϵ_m are the molar extinction coefficients of X_n and X_m. At a given temperature, the quantities A and ϵ_f are, of course, functions of wavelength and concentration while ϵ_n and ϵ_m are functions of wavelength alone. Equations (1) and (2) may be combined to eliminate one concentration variable.

Inasmuch as we have no direct way of measuring separately the two terms on the right-hand side of Eq. (2), we shall recast this equation into a form in which ϵ_n and ϵ_m are replaced by the formal extinction coefficients ϵ_f of two solutions which we can measure and which we shall call "reference" solutions. In choosing reference solutions we require only that the algebraic difference between their formal extinction coefficients be significantly larger than experimental errors over most of the wavelength range.

Designate quantities pertaining to the two reference solutions by the subscripts 1 and 2 and quantities pertaining to any other solution by the subscript 0. From Eq. (2) we have

$$(A/b)_0 = M_{f0}\epsilon_{f0} = M_{n0}\epsilon_{n0} + M_{m0}\epsilon_m \tag{3a}$$

$$(A/b)_1 = M_{f1}\epsilon_{f1} = M_{n1}\epsilon_n + M_{m1}\epsilon_m \tag{3b}$$

$$(A/b)_2 = M_{f2}\epsilon_{f2} = M_{n2}\epsilon_n + M_{m2}\epsilon_m. \tag{3c}$$

Define two parameters γ and δ by the equations

$$M_{n0} = \gamma M_{n1} + \delta M_{n2} \tag{4a}$$

$$M_{m0} = \gamma M_{m1} + \delta M_{m2}. \tag{4b}$$

Algebraic manipulation of Eqs. (3) and (4) leads to

$$(A/b)_0 = M_{f0}\epsilon_{f0} = \gamma M_{f1}\epsilon_{f1} + \delta M_{f2}\epsilon_{f2} \ . \tag{5}$$

Using Eqs. (1) and (4), the parameter δ may be eliminated by the relation

$$\delta = (M_{f0}/M_{f2}) - \gamma(M_{f1}/M_{f2}) \ . \tag{6}$$

The parameter γ may be expressed in terms of concentration variables by solving Eq. (4) to give

$$\gamma = (M_{m0}M_{n2} - M_{n0}M_{m2})/(M_{m1}M_{n2} - M_{n1}M_{m2}) \ . \tag{7}$$

Upon substituting Eqs. (6) and (7) into Eq. (5) and rearranging, we obtain

$$(\epsilon_{f0} - \epsilon_{f2}) = (\epsilon_{f1} - \epsilon_{f2})\,\gamma M_{f1}/M_{f0} \ . \tag{8}$$

Equation (8) may be somewhat generalized to give

$$(\epsilon_{f0} - \epsilon_{f1}) = (\epsilon_{f2} - \epsilon_{f3})\,\gamma_{021}\,\gamma_{132}\,M_{f2}\,M_{f3}/(M_{f0}\,M_{f1}) \tag{9}$$

where the subscripts 0, 1, 2, and 3 designate any four solutions, none of which need be regarded as references, and where

$$\gamma_{ijk} = (M_{mi}\,M_{nk} - M_{ni}\,M_{mk})/(M_{mj}\,M_{nk} - M_{nj}\,M_{mk}) \ . \tag{10}$$

We shall generally use these equations in the logarithmic forms

$$\log(\epsilon_{f0} - \epsilon_{f2}) = \log(\epsilon_{f1} - \epsilon_{f2}) + \log(\gamma M_{f1}/M_{f0}) \tag{11}$$

$$\log(\epsilon_{f0} - \epsilon_{f1}) = \log(\epsilon_{f2} - \epsilon_{f3}) + \log\zeta \tag{12}$$

where ζ is the collection of concentration terms in Eq. (9).

Equations (8), (9), (11), and (12) are alternative descriptions of the behavior of an isothermal family of spectra of solutions of two light-absorbing species in equilibrium which obey the law of additive absorbances. They will be referred to as the two-species model. In principle, ϵ_n/D_n and ϵ_m/D_m constitute the envelopes or extremes of an isothermal family, and all possible spectra of mixtures, that is, all ϵ_f, lie intermediate to these extremes.

There are two simple properties of the two-species model which may be deduced from the above equations and which serve as tests of the compliance of real solutions. First, if two spectra intersect at any point of the ϵ_f - λ plane, then all spectra intersect at this same point. This is the familiar isosbestic point which has long been used as a test of the two-species model. Unfortunately, the spectral range in our measurements is not wide enough to include an isosbestic point. Second, according to Eq. (12), $\log(\epsilon_{fi} - \epsilon_{fj})$ is, to within an additive constant, an invariant function of wavelength for every pair of spectra, ϵ_{fi} and ϵ_{fj}. This function is singular at isosbestic points and, hence, is of no practical value for wavelength regions where the ϵ_f curves come close together. For this reason, the above two properties are complementary tests of compliance. In the research described here, there are no isosbestic points and, hence, this conventional test is of no aid. For this reason, the second test was developed.

The extent to which the above compliance tests are unique for the two-species model may be ascertained by examining the N-species model. The above procedure for deriving the two-species model is easily generalized for N species in terms of N-reference solutions and gives

$$(A/b)_0 = M_{fo} \, \epsilon_{fo} = \sum_{j=1}^{N} \gamma_j \, M_{fj} \, \epsilon_{fj} \tag{13}$$

where M_{fj} and ϵ_{fj} are the M_f and ϵ_f of the j-th reference solution and γ_j is one of the N parameters which are functions of the concentrations of the N species. Any one and only one γ_j may be eliminated by the relation

$$M_{fo} = \sum_{j=1}^{n} \gamma_j \, M_{fj} \; . \tag{14}$$

By substituting the conditions of the compliance tests for the two-species model (for example, $\epsilon_{f1} = \epsilon_{f2} = \ldots = \epsilon_{fn}$ at an isosbestic point) into Eq. (13) and combining with Eq. (14), it may be shown that the multi-species models ($N > 2$) will not, in general, accord with these tests

and that an "accidental" accord is possible only for certain unique situations. The situations which give $\log(\epsilon_{fi} - \epsilon_{fj})$ an invariant shape for N greater than two are sufficiently unique so that we regard them as implausible.

It may be worth noting that the equations derived above apply to any solution of two solutes which are in equilibrium or which may be derived in principle from a common substance.

The experimental spectra at each temperature were tested by computing $\log(\epsilon_{fi} - \epsilon_{fj})$ over the full wavelength range for many pairs of ϵ_f functions, and then verifying that the shapes of the resultant curves were essentially the same. An example of the results is shown in Fig. 6 by a systematic set of $\log(\epsilon_{fi} - \epsilon_{fj})$ functions for 264°C. It will simplify discussion to denote the spectrum ϵ_{fi} of the solution with concentration M_{fi} as $\epsilon_f\langle M_{fi}\rangle$. In Fig. 6 two spectra serve as references. These are $\epsilon_f\langle 0.696\rangle$, the spectrum of the solution of greatest M_f, and $\epsilon_f\langle 0.0118\rangle$, a representative spectrum from the linear A/b - M_f range. From these reference spectra, the reference function $\log(\epsilon_f\langle 0.0118\rangle - \epsilon_f\langle 0.696\rangle)$ was computed and is plotted twice in Fig. 6 as curves A and E. This reference function may be thought of as a standard shape against which the shapes of the other curves are compared. All of the remaining spectra at 264°C were divided into two groups. One group, those with low concentrations, was referenced against $\epsilon_f\langle 0.696\rangle$ to give the set of functions $\log(\epsilon_f\langle M_{fi}\rangle - \epsilon_f\langle 0.696\rangle)$ which are plotted in Fig. 6 as curves A through D. The other group, those with high con-centrations, was referenced against $\epsilon_f\langle 0.0118\rangle$ to give the set of functions $\log(\epsilon_f\langle 0.0118\rangle - \epsilon_f\langle M_{fi}\rangle)$ which are plotted as curves E through L. These two groups overlap, for example, $\epsilon_f\langle 0.0341\rangle$ was referenced against $\epsilon_f\langle 0.696\rangle$ to give curve C and against $\epsilon_f\langle 0.0118\rangle$ to give curve K. Spectra for solutions of quite high M_f were not referenced against $\epsilon_f\langle 0.696\rangle$ because the difference $(\epsilon_f\langle M_{fi}\rangle - \epsilon_f\langle 0.696\rangle)$ is a small number that contains a large relative error which is further exaggerated by taking the logarithm. This consideration obviously applies likewise to the spectra of solutions of quite low M_f referenced against $\epsilon_f\langle 0.0118\rangle$. In the latter case, the magnitude of errors may be visualized from the spectra shown in Fig. 2. In particular, the difference
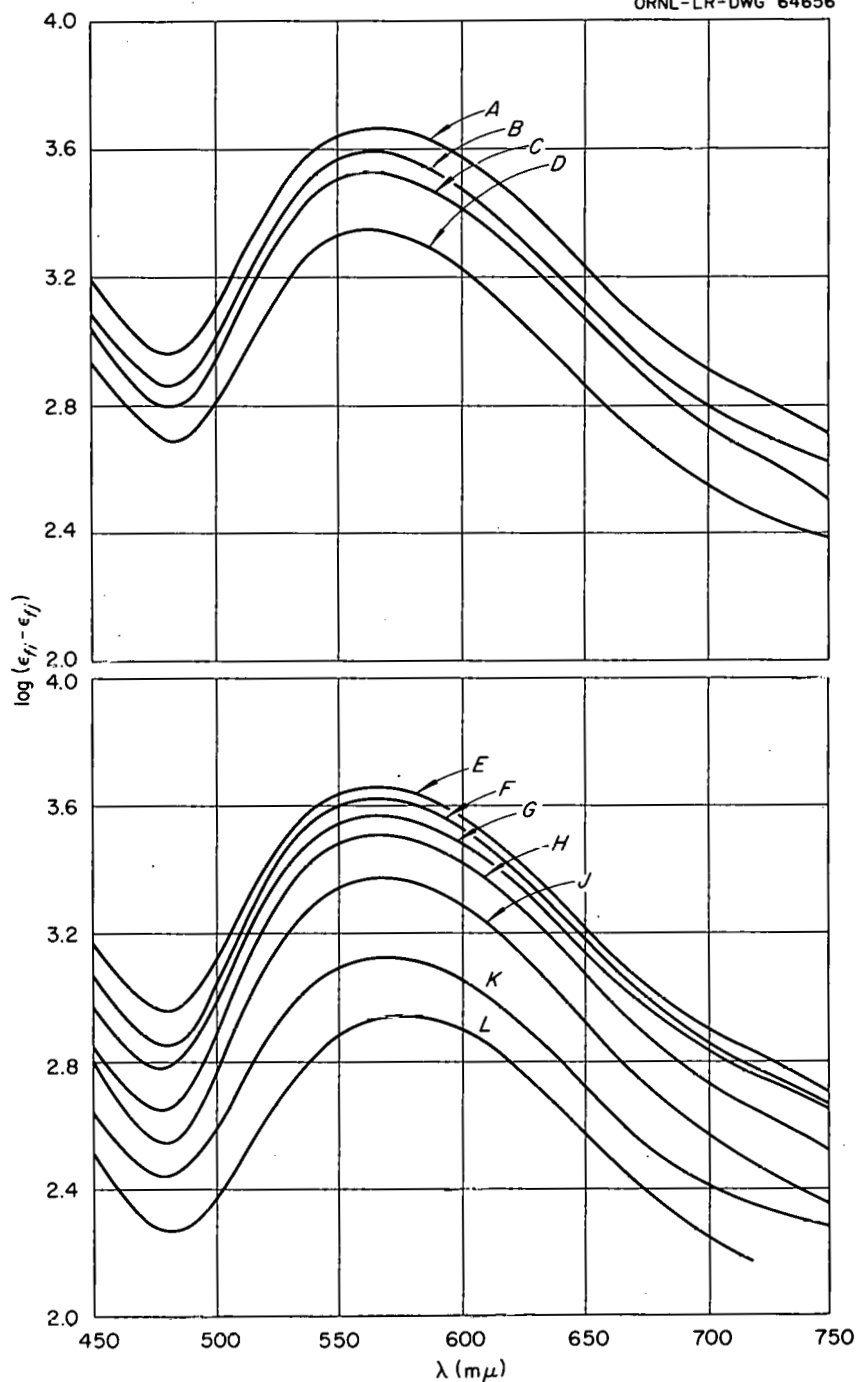
Fig. 6. Test of the Agreement Between the Observed Spectra at $264°C$ and the Two-Species Model. Curves A and E are identical. For curves A through D, M_{fi} is 0.696 and M_{fj} is as follows: A = 0.0118, B = 0.0248, C = 0.0341, and D = 0.0595. For curves E through L, M_{fi} is 0.0118 and M_{fj} is as follows: E = 0.696, F = 0.295, G = 0.156, H = 0.113, J = 0.0632, K = 0.0341, and L = 0.0248.

$(\epsilon_f\langle 0.0118\rangle - \epsilon_f\langle M_{fi}\rangle)$ must be chosen to be large relative to the width of the shaded strip in Fig. 2. Of course, the difference between any two $\epsilon_f\langle M_{fi}\rangle$ for concentrations within the linear A/b - M_f region (shaded strip) produces curves of meaningless shape which contain only experimental errors.

For the curves shown in Fig. 6, several sources of error should be noted. At wavelengths near 750 mμ, the $\epsilon_f\langle M_{fi}\rangle$ draw closely together and their differences contain a large relative error. At wavelengths greater than 500 mμ, the spectra at low concentrations, which were measured at long path lengths, contain a relatively large error arising from errors in measuring the steeply rising spectrum of the $BiCl_3$ solvent as illustrated in Fig. 1 and discussed in the Results section. These sources of error increase considerably at higher temperatures. Finally, the spectra for high bismuth concentrations were measured in cells with path lengths of the order of 24 μ. Such short path lengths are difficult to measure precisely and path-length errors become aggravated in taking the difference between two $\epsilon_f\langle M_{fi}\rangle$ of widely different M_f since each $\epsilon_f\langle M_{fi}\rangle$ is necessarily measured at a substantially different path length.

The curves shown in Fig. 6 closely approximate the same shape. The largest deviations occur, as expected, at the wavelength extremes. Most important, deviations from the standard shape of curves A and E show no trend with changing M_f such as would indicate the growing in of a third solute species.

The curves in Fig. 6 do not represent all of the spectra at 264°C. The omitted spectra, which correspond to fairly high and fairly low M_f values, give $\log(\epsilon_f\langle 0.0118\rangle - \epsilon_f\langle M_{fi}\rangle)$ or $\log(\epsilon_f\langle M_{fi}\rangle - \epsilon_f\langle 0.696\rangle)$ functions which lie quite close to functions which are shown and could not be included in Fig. 6 without confusion.

Other families of functions like those in Fig. 6 were computed by using other spectra as references. All such functions at 264°C yielded curves of substantially the same shape as shown in Fig. 6.

The same tests were applied to the spectra at 350 and 433°C and at each temperature the only significant difference between different $\log(\epsilon_f\langle M_{fi}\rangle - \epsilon_f\langle M_{fj}\rangle)$ functions was a linear displacement. Deviations

between the shape of a reference function and other functions increased somewhat with increasing temperature, but these differences showed no trend with a systematic change in M_f which would indicate the growing in of a third solute species.

CONCLUSION

The data presented here provide substantial evidence that, in dilute solutions of bismuth metal in fused $BiCl_3$, the solute exists as two light-absorbing species.

ACKNOWLEDGMENT

THIS PAGE

WAS INTENTIONALLY

LEFT BLANK

ORNL-3316
UC-25 — Metals, Ceramics, and Materials
TID-4500 (17th ed., Rev.)

INTERNAL DISTRIBUTION

1. Biology Library
2-3. Central Research Library
4. Laboratory Shift Supervisor
5. Reactor Division Library
6-7. ORNL — Y-12 Technical Library
    Document Reference Section
8-27. Laboratory Records Department
28. Laboratory Records, ORNL R.C.
29. G. M. Adamson, Jr.
30. P. A. Agron
31. M. Blander
32. F. F. Blankenship
33. B. S. Borie
34. C. R. Boston
35. M. A. Bredig
36. H. R. Bronstein
37. J. H. Crawford, Jr.
38. J. E. Cunningham
39. M. D. Danford
40. D. A. Douglas, Jr.
41. J. H. Frye, Jr.
42-46. M. R. Hill
47. D. W. James

48. R. G. Jordan (Y-12)
49. H. W. Joy
50. C. E. Larson
51. H. A. Levy
52. C. H. Liu
53. H. G. MacPherson
54. W. D. Manly
55. C. J. McHargue
56. J. P. Murray (K-25)
57. P. Patriarca
58. R. M. Rush
59. M. J. Skinner
60-69. G. P. Smith, Jr.
70. J. A. Swartout
71. W. C. Waggener
72. A. M. Weinberg
73. J. C. White
74. J. C. Wilson
75. J. P. Young
76. A. A. Burr (consultant)
77. J. R. Johnson (consultant)
78. C. S. Smith (consultant)
79. R. Smoluchowski (consultant)

EXTERNAL DISTRIBUTION

80-81. David F. Cope, Oak Ridge Operations Office
82. D. E. Baker, General Electric, Hanford
83. Ersel Evans, General Electric, Hanford
84. J. L. Gregg, Cornell University
85. J. Simmons, Atomic Energy Commission, Washington
86. Lawrence M. Slifkin, University of North Carolina
87. E. E. Stansbury, University of Tennessee
88. Donald K. Stevens, Atomic Energy Commission, Washington
89. Division of Research and Development, AEC, ORO
90-588. Given distribution as shown in TID-4500 (17th ed., Rev.) under
    Metals, Ceramics, and Materials category